

# Discovery and photometry of the binary-lensing caustic-crossing event EROS-BLG-2000-5

C. Afonso<sup>1,8</sup>, J.N. Albert<sup>2</sup>, J. Andersen<sup>6</sup>, R. Ansari<sup>2</sup>, É. Aubourg<sup>1</sup>, P. Bareyre<sup>1,4</sup>, G. Blanc<sup>1</sup>, X. Charlot<sup>1</sup>, F. Couchot<sup>2</sup>, C. Coutures<sup>1</sup>, R. Ferlet<sup>5</sup>, D. Fields<sup>7</sup>, P. Fouqué<sup>9,10</sup>, J.F. Glicenstein<sup>1</sup>, B. Goldman<sup>1,8</sup>, A. Gould<sup>7</sup>, D. Graff<sup>7</sup>, M. Gros<sup>1</sup>, J. Haïssinski<sup>2</sup>, C. Hamadache<sup>1</sup>, J. de Kat<sup>1</sup>, L. LeGuillou<sup>1</sup>, É. Lesquoy<sup>1,5</sup>, C. Loup<sup>5</sup>, C. Magneville<sup>1</sup>, J.B. Marquette<sup>5</sup>, É. Maurice<sup>3</sup>, A. Maury<sup>9</sup>, A. Milsztajn<sup>1</sup>, M. Moniez<sup>2</sup>, N. Palanque-Delabrouille<sup>1</sup>, O. Perdereau<sup>2</sup>, L. Prévot<sup>3</sup>, Y. Rahal<sup>2</sup>, J. Rich<sup>1</sup>, M. Spiro<sup>1</sup>, P. Tisserand<sup>1</sup>, A. Vidal-Madjar<sup>5</sup>, L. Vigroux<sup>1</sup>, S. Zylberajch<sup>1</sup>  
The EROS collaboration

<sup>1</sup> CEA, DSM, DAPNIA, Centre d'Études de Saclay, F-91191 Gif-sur-Yvette Cedex, France

<sup>2</sup> Laboratoire de l'Accélérateur Linéaire, IN2P3 CNRS, Université de Paris-Sud, F-91405 Orsay Cedex, France

<sup>3</sup> Observatoire de Marseille, 2 pl. Le Verrier, F-13248 Marseille Cedex 04, France

<sup>4</sup> Collège de France, Physique Corpusculaire et Cosmologie, IN2P3 CNRS, 11 pl. M. Berthelot, F-75231 Paris Cedex, France

<sup>5</sup> Institut d'Astrophysique de Paris, INSU CNRS, 98 bis Boulevard Arago, F-75014 Paris, France

<sup>6</sup> Astronomical Observatory, Copenhagen University, Juliane Maries Vej 30, DK-2100 Copenhagen, Denmark

<sup>7</sup> Departments of Astronomy and Physics, Ohio State University, Columbus, OH 43210, U.S.A.

<sup>8</sup> Department of Astronomy, New Mexico State University, Las Cruces, NM 88003-8001, U.S.A.

<sup>9</sup> European Southern Observatory, Casilla 19001, Santiago 19, Chile

<sup>10</sup> Observatoire de Paris-Meudon LESIA, F92195 Meudon CEDEX, France

Received , accepted

**Abstract.** The EROS collaboration has developed a real time alert system, which was operational in 1999 and 2000. A very long binary-lensing caustic crossing event, EROS-BLG-2000-5, was found in the 2000 season and monitored by EROS. EROS photometric data for this event are presented. The data are well fitted by the model of An et al. (2002) based on a completely different dataset. However, parameters of the model such as the mass ratio or the binary rotation rate are not very well constrained by EROS data.

**Key words.** gravitational lensing – techniques: alert systems – stars: atmospheres

## 1. Introduction

Micro-lensing is becoming established as a powerful tool in astrophysics. Astrophysical information on the source can often be obtained even with only limited information on the geometry of the lens. For instance, the spatial structure of the atmosphere can be studied when a lens caustic passes over the face of a source. For point lenses, the caustics are point-like, so that the probability of such a crossing is small. For binary lenses, the caustics form one to three polygon-shaped curves and the probability of crossing is of the order of a few percent. Caustics are generic singularities of the lens mapping (“catastrophes”). Because of this, the shape of the microlensing light curve is accurately described by a limited number of parameters (including limb darkening parameters), almost independently of the lens model. Intensive photometric observations of four binary caustic crossing events have yielded limb-darkening measurements (Afonso et al. 2000; Albrow et al. 1999, 2000, 2001a).

The implementation of alert systems by all the major microlensing surveys: OGLE (Udalski et al. 1994), MACHO (Alcock et al. 1996), EROS and the MOA collaboration (Bond et al. 2001) was the key improvement. These collaborations issued hundreds of microlensing alerts, found mostly towards the Galactic Bulge. The EROS microlensing alert system, which is described in the first part of this paper, was mainly operational during the 1999 and the 2000 seasons. An interesting binary-lensing caustic crossing event, EROS-BLG-2000-5, was found during the 2000 season. This event was intensively monitored by various “follow-up” collaborations such as PLANET<sup>1</sup> and MPS<sup>2</sup> and also by EROS. High resolution spectra were taken on the

Send offprint requests to: J-F. Glicenstein

<sup>1</sup> <http://thales.astro.rug.nl/planet/>

<sup>2</sup> <http://bustard.phys.nd.edu/MPS/index.html>

Keck during the second caustic crossing by Castro et al. (2001). Lower resolution spectra were obtained on the VLT by Albrow (2001b). These groups detected a significant evolution of the equivalent width of the  $H\alpha$  line during the crossing. Afonso et al. (2001) reanalyzed the spectral data using a subsample of EROS photometric data. They found evidence for chromospheric activity of the K3 giant source. A detailed lens model of EROS-BLG-2000-5 was published by An et al. (2002). The measurement of both the finite size of the source and the effect of Earth motion (“parallax”) allowed the simultaneous determination of the lens distance, transverse velocity and mass. An and co-authors studied limb darkening only for the I passband. However, the second caustic crossing of EROS-BLG-2000-5 was monitored in 3 passbands by PLANET and 2 other passbands by EROS. This allows a precise comparison between the observed limb darkening and the prediction of various atmospheric models (Fields et al. 2003). The extraction of limb darkening parameters relies on the agreement between the lens model of An et al. (2002) and PLANET data. The photometric data reduction for EROS-BLG-2000-5, and the comparison to the lens model of An et al. (2002) is reported in the second part of the paper.

## 2. The EROS survey and alert system

The EROS project used a dedicated 1 meter telescope and two 1 deg<sup>2</sup> cameras at the La Silla ESO site to monitor fields in the Magellanic Clouds, the Galactic Bulge and the Galactic Disc. The detector setup is described in detail in Bauer & de Kat (1996) and the data acquisition system in Glicenstein & Gros (1998). Sixty to eighty images were taken every night and flat-fielded online. EROS observations were carried out in two bands  $V_E$  and  $I_E$ . EROS  $V_E$  is centered midway between Johnson  $V$  and Cousins  $R$ , while EROS  $I_E$  is similar to Cousins  $I$ , but broader. More precisely

$$V_E = 0.69 V + 0.31 I, \quad I_E = -0.01 V + 1.01 I, \quad (1)$$

(Regnault 2000). The disc capacity of the acquisition computers was sufficient for storing roughly one night of data taking. The data were then copied to tapes and sent to Lyon (France) for offline analysis at the high energy physics computing centre (CC-IN2P3). Two dedicated computers were installed on site to perform real-time photometry on a limited set of EROS fields. This set included all the EROS Small Magellanic Cloud (SMC) fields ( $\sim 9$  deg<sup>2</sup>) and roughly one third ( $\sim 22$  deg<sup>2</sup>) of the Galactic Bulge (BLG) fields. Five million stars were thus monitored towards the SMC. Two novæ were discovered and reported (Glicenstein 1999a,b). Only 4.3 million bright stars were monitored towards the Galactic Bulge. This bright star sample was selected to minimize the blending of source stars and to disentangle the various (disc, bulge) contributions to the microlensing optical depth towards the Galactic Centre (Gould 1995; Afonso et al. 2003). The sampling rate for these fields ranges from one image every 1-4 nights for the SMC fields to one image every night for some of the BLG fields.

The online photometry and alert system is controlled by Perl scripts. Each of the scripts in turn calls C++ programs written with the PEIDA++ class library. The system operation can be split into four basic tasks.

The first task starts at the end of every night of data taking and makes lists of images to be processed by the photometry (second) task. The latter is similar to the offline photometric reduction. It uses our standard PEIDA (Ansari 1996) PSF-based software. The star catalogues are copies of the offline catalogues. The output of the photometric reduction had to be simplified to save disc space. Since we had a limited disc storage capacity on site, the photometric reduction had to run in less than a few hours. The time needed to process a full image of 8 CCD was of the order of 15 minutes (both colours running in parallel). The number of alert fields was restricted to  $\sim 40$  fields both by the disc capacity and the available CPU power.

The third task is the detection of potential ongoing microlensing events (“trigger”). This was done by comparing the template flux of each star in the catalogue to the measured flux. The template fluxes and the typical photometric errors were computed offline using  $\sim 60$  measurements taken during the first 2 years of data taking. The “trigger” task first builds the light curve in  $I_E$  and  $V_E$  of each star in the catalogue. This light curve contains only data points from the running season. Quality cuts are then applied to remove data points with large absorption, seeing or skylight. A “trigger condition” arises when a star shows a significant deviation from its template flux simultaneously in both passbands. The distribution of deviations from the template flux is not distributed as a gaussian. Relatively large deviations may occur because of systematic errors in the photometry (e.g. small errors in the position of sources in the catalogue) or poor data taking conditions (e.g. large airmasses). Various “trigger conditions” have been tried. Examples are 4 points in a row at more than 4 times the photometric error, 1 point in both colors at more than 7 times the photometric error and a minimum increase in flux. The trigger task logs the information (position, flux, trigger conditions) of stars that satisfy at least one trigger condition to a file.

The last task builds the light curves of all the candidate microlensing events. These candidates are scanned by eye to remove obvious photometric problems (such as noisy pixels or contamination by the light of a nearby luminous star) and finally are run through more sophisticated tests. The colour of the source is compared to the position of the red giant clump on the local colour-magnitude diagram. Sources redder than the red giant clump, which often show long term time variations which may fake microlensing are rejected. Finally, the light curve is fitted to a “point lens-point source” (PLPS) lens model. The latter (Paczynski 1986) is defined by:

$$F^p(t) = A(t)F_s^p + F_b^p \quad (2)$$

$$A = \frac{u^2+2}{u\sqrt{u^2+4}} \quad (3)$$

**Table 1.** EROS data on EROS-BLG-2000-5

filter	images	images after quality cut	selected for fit	error renormalization factor
$V_E$	1275	1021	830	1.24
$I_E$	1207	904	904	1.16

$$u^2 = u_o^2 + \left(\frac{t-t_o}{t_E}\right)^2 \quad (4)$$

where  $F^p$ ,  $F_s^p$ ,  $F_b^p$  are the total, source and background fluxes in passband  $p$ , measured at time  $t$  and  $t_E$  is the Einstein radius crossing time. The maximum amplification  $A_{max}$  of the background source occurs at time  $t_o$ . Light curves with  $A_{max} < 1.3$  are rejected.

An alert is sent to a mail distribution list when the candidate passes all the tests. Information on the event such as the coordinates of the source, finding charts, colour-magnitude diagrams and parameters of the PLPS fit are displayed on a Web page<sup>3</sup>. Fifteen microlensing alerts were sent during the 1999 and the 2000 seasons. Seven other events were found in 1998 and 2001.

EROS BLG data of the 1996,1997 and 1998 seasons have been analyzed by Afonso et al. (2003). These authors found sixteen microlensing events with red giant sources and a maximum amplification  $A_{max} > 1.34$ . The four microlensing alerts of the 1998 season were also found by Afonso et al. (2003). However, one of these alerts had  $A_{max} = 1.32$  and thus was not included in the final offline sample. Roughly 20% of the alerts given by the EROS alert system in 1999 and 2000 were probable variable stars. Accounting for the smaller efficiency of data taking during the first years of EROS2, the rate of online microlensing events detection is typically half of the offline detection rate (Afonso et al. 2003).

### 3. EROS-BLG-2000-5

This event was alerted by EROS on 5 May 2000. On 8 June 2000, MPS issued an anomaly alert, informing that a caustic crossing was in progress. Subsequent intensive observations by PLANET allowed them to predict the time of the second caustic crossing and, very importantly, that this crossing would last an unusually long 4 days. The event was densely monitored by EROS. EROS observations are normally carried out in survey mode, but owing to the importance of the event, extra time was allocated to it. Between the caustic crossings, images were taken whenever possible, even on cloudy nights or nights affected by moon light. During the second crossing, all available time was allocated to it.

#### 3.1. Photometric Data

The EROS images have been reprocessed using the ISIS (Alard 2000) image subtraction program on a small 300x300 vignette around the source star. The online PEIDA photometry was used to obtain the zero point of image subtracted photometry as explained in Afonso et al. (2001) (see their figure 4). All the images were sent through the photometry pipeline. However, some images were of low quality and the photometry showed a large dispersion (figure 1 a). The dispersion was reduced by using a quality factor. This quality factor is simply the number of stars  $n_{star}$  reconstructed on the vignette around the source star. The effect of  $n_{star}$  on the photometric dispersion is illustrated on figure 1. Typical values for  $n_{star}$  on high quality data range from 250 to 400 on  $V_E$  data and from 200 to 250 on  $I_E$  data. To avoid losing too many points, somewhat looser cuts were adopted:  $n_{star} > 180$  on  $V_E$  data and  $n_{star} > 170$  on  $I_E$  data. The cut on  $n_{stars}$  is still fairly severe, as shown in table 1. Only roughly two thirds of the points survive the cuts. The photometric error can be estimated from the dispersion in the high quality data. Ideally, the photometric dispersion after the quality cut should be given by the photon noise. However, it is found to be slightly larger. The true photometric error is obtained from the photon noise dispersion by multiplying by the numbers in the fifth column of table 1.

#### 3.2. Lens model and discussion

Our data have been fitted to a variant of the model of An et al. (2002). This model takes into account both the finite size of the source (through the projection of the source star on the lens plane  $\rho_*$ ), and the two components of projected motion of the Earth on the lens plane (“parallax”)  $\pi_{E,\parallel}$  parallel and  $\pi_{E,\perp}$  perpendicular to the binary axis. The geometry of the various projections is shown in figure 2 of An et al. (2002). The other parameters are the time of closest approach to the cusp  $t_c$ , the distance  $d_c$  of the 2 components of the binary evaluated at  $t_c$ , the time variation of this distance  $\dot{d}$ , the mass ratio  $q$ , the distance of closest approach  $u_c$ , the Einstein radius crossing time  $t'_E$ , the angle between the lens trajectory and the binary axis  $\alpha'$  and the binary rotation rate

<sup>3</sup> <http://www-dapnia.cea.fr/Spp/Experiences/EROS/alertes.html>

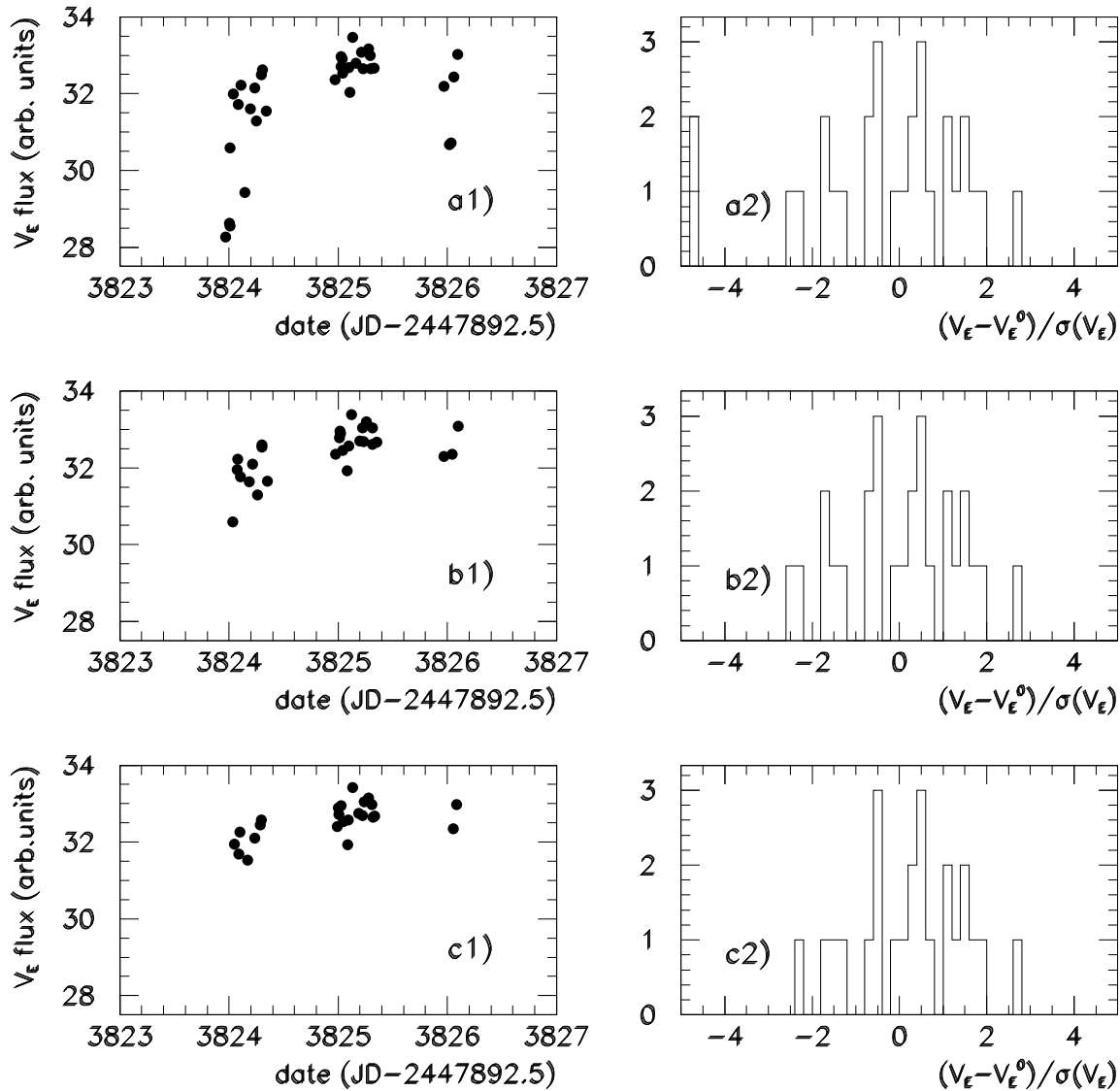


**Fig. 1.** EROS  $V_E$  data between JD 2451715.5 and JD 2451719.5. Plots on the left panel show the light curves and plots on the right panel show the photometric dispersion. The quality cut is increasingly demanding from top to bottom. a) all measurements ( 34 points) b) measurements with  $n_{\text{star}} > 180$  (28 points) c) measurements with  $n_{\text{star}} > 250$  (24 points).  $V_E^o$  is the average  $V_E$  flux calculated with  $n_{\text{star}} > 180$ .  $\sigma(V_E)$  is the ISIS photometry error.

$\omega$ . The total number of geometric parameters is thus 11. There are also 4 additional parameters per passband: the source flux, the background flux and 2 limb darkening parameters. In the original An et al. model, only I passband was used, but the images came from several observatories. Because of this, a different source flux, background flux and seeing correction had to be fitted for each observatory.

The fitting procedure is described in detail in An et al. (2002) and Fields et al. (2003). The minimum  $\chi^2$  is found by stepping over a grid of  $(d_{lc}, q)$  values and minimizing over the other parameters. The apparent  $\chi^2$  surface has a very complicated and “rough” shape around the minimum as explained in Fields et al. (2003). Multiple local minima are possible. The numerical evaluation of errors is made difficult by the roughness of the  $\chi^2$  surface.

EROS  $V_E$  and  $I_E$  data are displayed in figures 2 and 3. The An et al. (2002) lens model, which is superimposed on the data, gives obviously an excellent fit. The location of the second caustic exit is clearly seen in EROS data (see figure 4) and is in very

**Table 2.** Parameters of lens models for EROS-BLG-2000-5. The fit errors were not calculated for models 1 and 2 because of numerical problems (see Fields et al. (2003)). The last two columns are taken from An et al. (2002) table 3.

Parameter	Model 1 Value	Model 2 Value	An et al Value	Uncertainty
$d_{tc}$	1.935	1.935	1.928	0.004
$q$	0.77	0.76	0.7485	0.0066
$\alpha'$ (deg)	73.82	73.62	74.18	0.41
$u_c$	$-5.11 \cdot 10^{-3}$	$-5.12 \cdot 10^{-3}$	$-5.2 \cdot 10^{-3}$	$3 \cdot 10^{-5}$
$t'_E$ (days)	100.9	99.7	99.8	1.5
$t_c$ (days)	3844.439	3844.438	3844.444	0.005
$\rho_*$	$4.88 \cdot 10^{-3}$	$4.92 \cdot 10^{-3}$	$4.80 \cdot 10^{-3}$	$4 \cdot 10^{-5}$
$\pi_{E,\parallel}$	-0.126	-0.164	-0.165	0.042
$\pi_{E,\perp}$	0.169	0.148	0.222	0.031
$\dot{d}$ (yr $^{-1}$ )	0.24	0.31	0.203	0.016
$\omega$ (yr $^{-1}$ )	-0.05	0.019	0.006	0.076
$\chi^2/d.o.f$	1712.1/(1734 - 19) 1713.8/(1734 - 19) 2255/(1734 - 19)			

good agreement with the prediction of the model. Note that this prediction was not tested in the An et al. (2002) paper because of the lack of data immediately after the end of the caustic crossing (see their section 3.2).

However, several other  $(d_{tc}, q)$  values are found to give excellent fits to the EROS data. Two examples of such fits (local minima of the apparent  $\chi^2$  surface), labelled “Model 1” and “Model 2” are shown in table 2 and compared to the An et al. (2002) values.

The residuals of the fit of model 1, normalized by the photometric errors, are shown in figures 5 and 6. These residuals do not show any systematic trend as a function of time. The distributions of residuals  $r_{V_E}$  and  $r_{I_E}$  are well fitted by gaussian distributions in both  $I_E$  and  $V_E$  filters. The widths  $\sigma(r_{V_E})$  and  $\sigma(r_{I_E})$  of the distributions are close to unity:

$$\sigma(r_{V_E}) = 0.86 \pm 0.03 \quad (5)$$

$$\sigma(r_{I_E}) = 1.07 \pm 0.03 \quad (6)$$

The prediction of model 1 is systematically smaller than the data in both passbands, but the difference is only  $\sim 1/10$  of the typical error bar. It is clear from table 2 that some parameters are not very well constrained by EROS data. The parameters  $q$  and  $\pi_{E,\perp}$  are mildly inconsistent with the values found by An et al. (2002), while the value of  $\dot{d}$  in model 2 is highly inconsistent.

#### 4. Summary

The binary-lensing caustic-crossing microlensing event EROS-BLG-2000-5 was found by the EROS alert system during the 2000 Bulge season. The EROS data are well fitted by the lens model of An et al. (2002). In particular, this model predicts the observed end of the second caustic crossing. However, EROS data are also consistent with other slightly different models. The combined fit of all EROS and PLANET data (Fields et al. 2003) should hopefully improve the situation.

*Acknowledgements.* We are grateful to D. Lacroix and the technical staff at the Observatoire de Haute Provence and to A. Baranne for their help with the MARLY telescope. We are also grateful for the support given to our project by the technical staff at ESO, La Silla. We thank J.F. Lecoince and A. Gomes for assistance with the online computing. Work by AG and DF was supported by NSF grant AST 02-01266.

#### References

- Afonso, C. et al. 2000, ApJ, 532, 340
- . 2001, A&A, 378, 1014
- . 2003, to be published in A&A(astro-ph/0303100)
- Alard, C. 2000, A&AS, 144, 363
- Albrow, M. et al. 1999, ApJ, 522, 1011
- . 2000, ApJ, 534, 894
- Albrow, M. et al. 2001a, ApJ, 549, 759
- . 2001b, ApJ, 550, L173

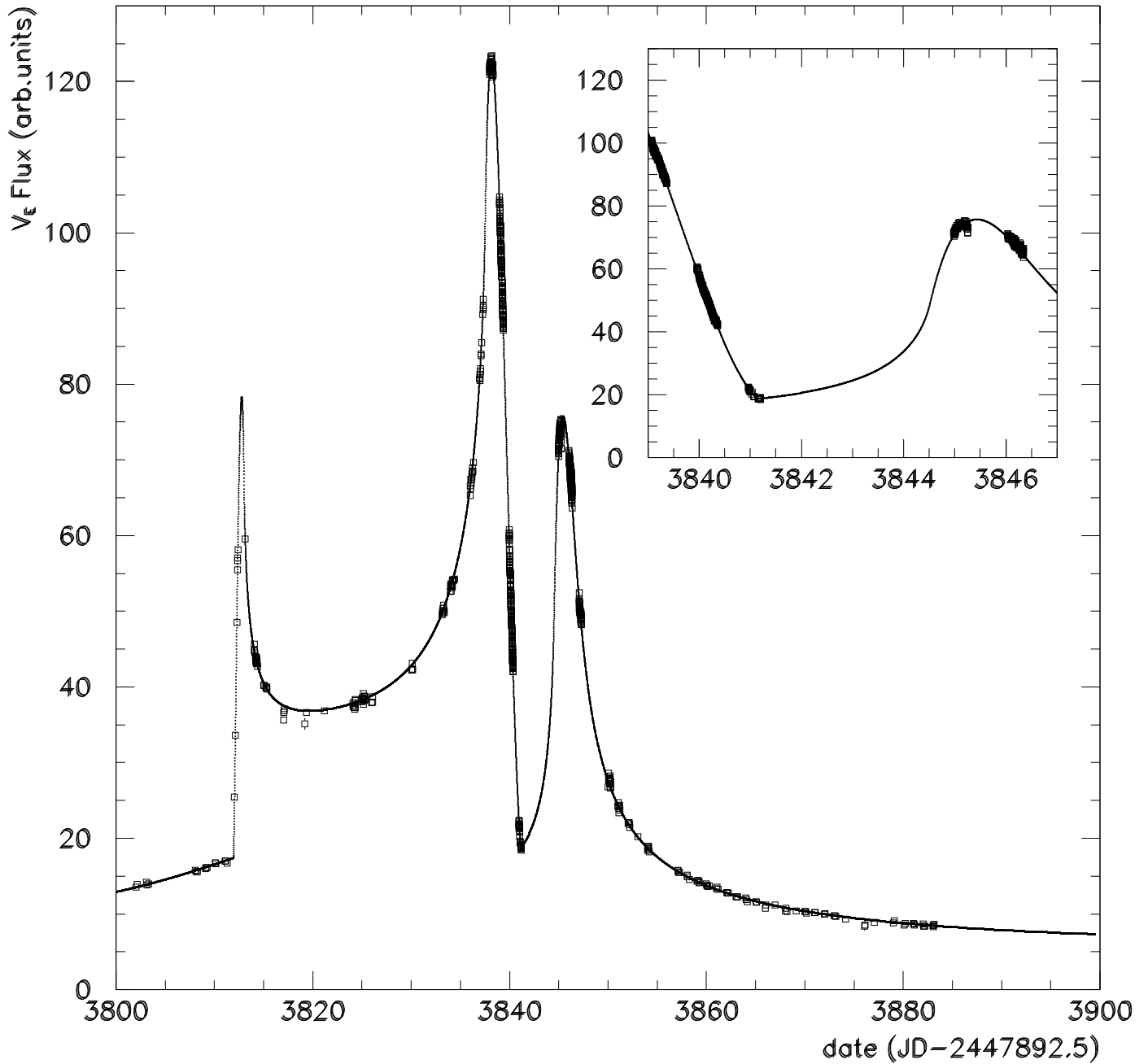


**Fig. 2.** EROS  $V_E$  data (squares) compared to the An et al. (2002) lens model (solid line). The blowup shows the end of the second caustic crossing and the cusp approach.

Alcock, C. et al. 1996, *ApJ*, 463, L67

An, J. et al. 2002, *ApJ*, 572, 521

Ansari, R. 1996, *Vistas in Astronomy*, 40, 519

Bauer, F. & de Kat, J. 1996, in *Optical Detectors for Astronomy* : J. W. Beletic & P. Amico eds.

Kluwer Academic Publishers, Boston, Mass., 1998

(Astrophysics and space science library), Vol. 228, 191

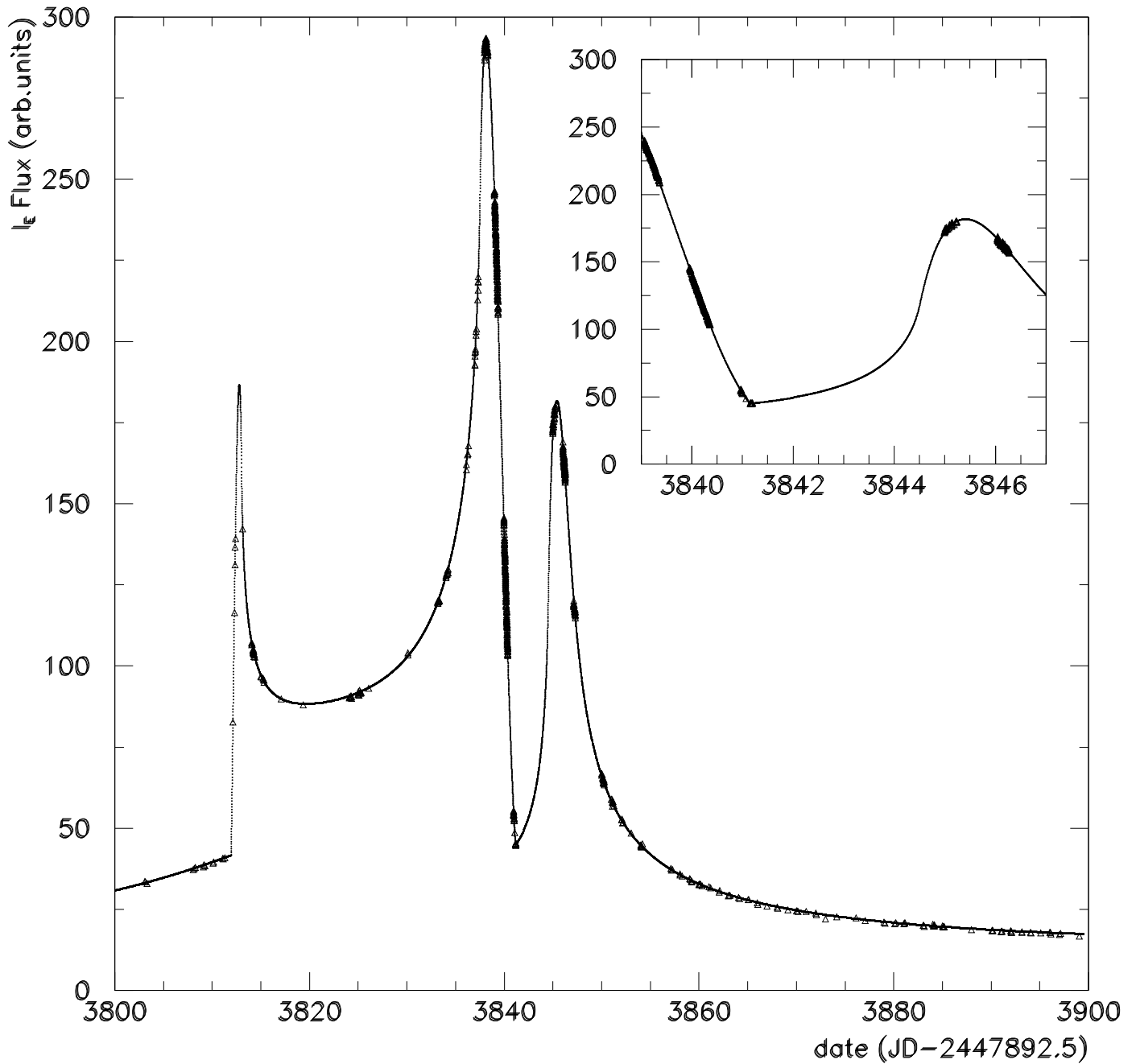


**Fig. 3.** EROS  $I_E$  data (triangles) compared to the An et al. (2002) lens model (solid line). The blowup shows the end of the second caustic crossing and the cusp approach.

Bond, I. et al. 2001, MNRAS, 327, 868

Castro, S. et al. 2001, ApJ, 548, L197

Fields, D. et al. 2003, in preparation

Glicenstein, J.-F. 1999a, IAUC 7236

—. 1999b, IAUC 7286

Glicenstein, J.-F. & Gros, M. 1998, IEEE transactions on nuclear science, 45, 1830

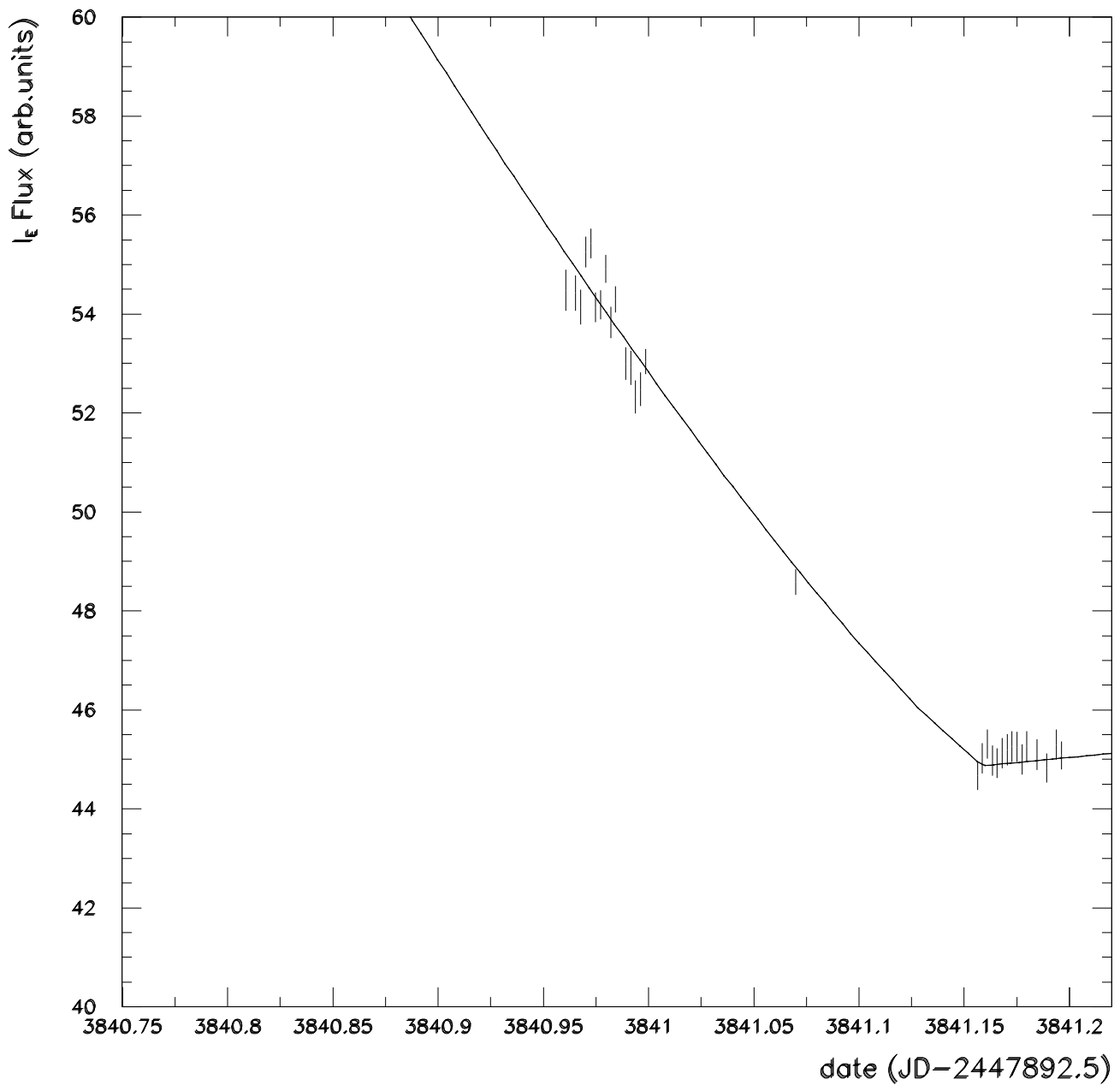


**Fig. 4.** Blowup of the exit of second caustic crossing for EROS  $I_E$  data. The solid line is the prediction of An et al. (2002). Note that this model is based on a dataset where the caustic exit was not observed.

Gould, A. 1995, ApJ, 447, 491

Paczynski, B. 1986, ApJ, 304, 1

Regnault, N. 2000, PhD thesis, Université de Paris 7 (LAL 00-65)

Udalski, A. et al. 1994, Acta Astronomica, 44, 227



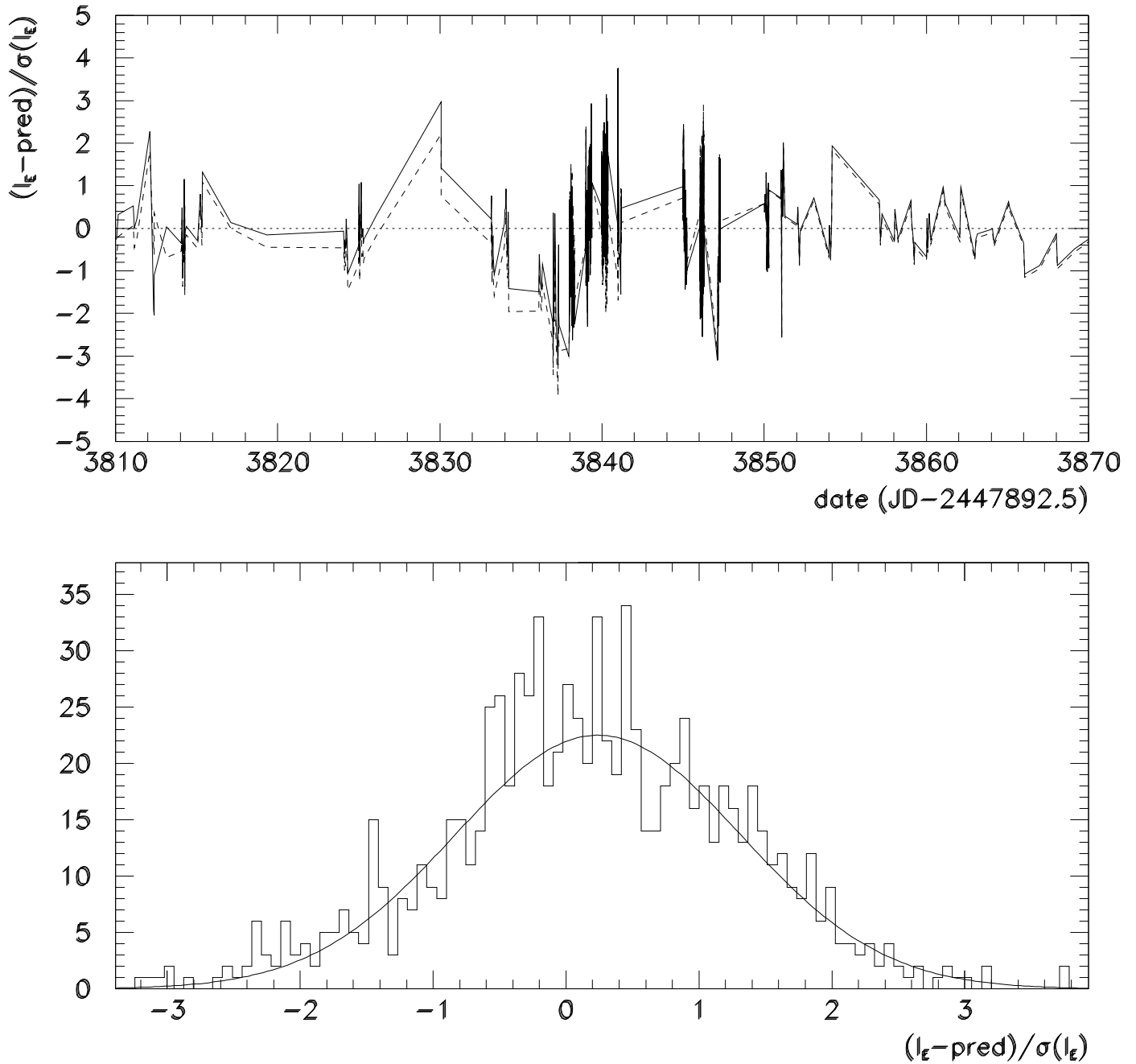


**Fig. 5.** Normalized residuals of EROS  $I_E$  data. Top: residuals as a function of time. The solid line is model 1 (model2 is not shown but similar) and the dashed line is An et al. (2002) lens model. The residuals of both models do not show any obvious trend as a function of time. Bottom: distribution of residuals for model 1. The solid line shows the fit to a gaussian.

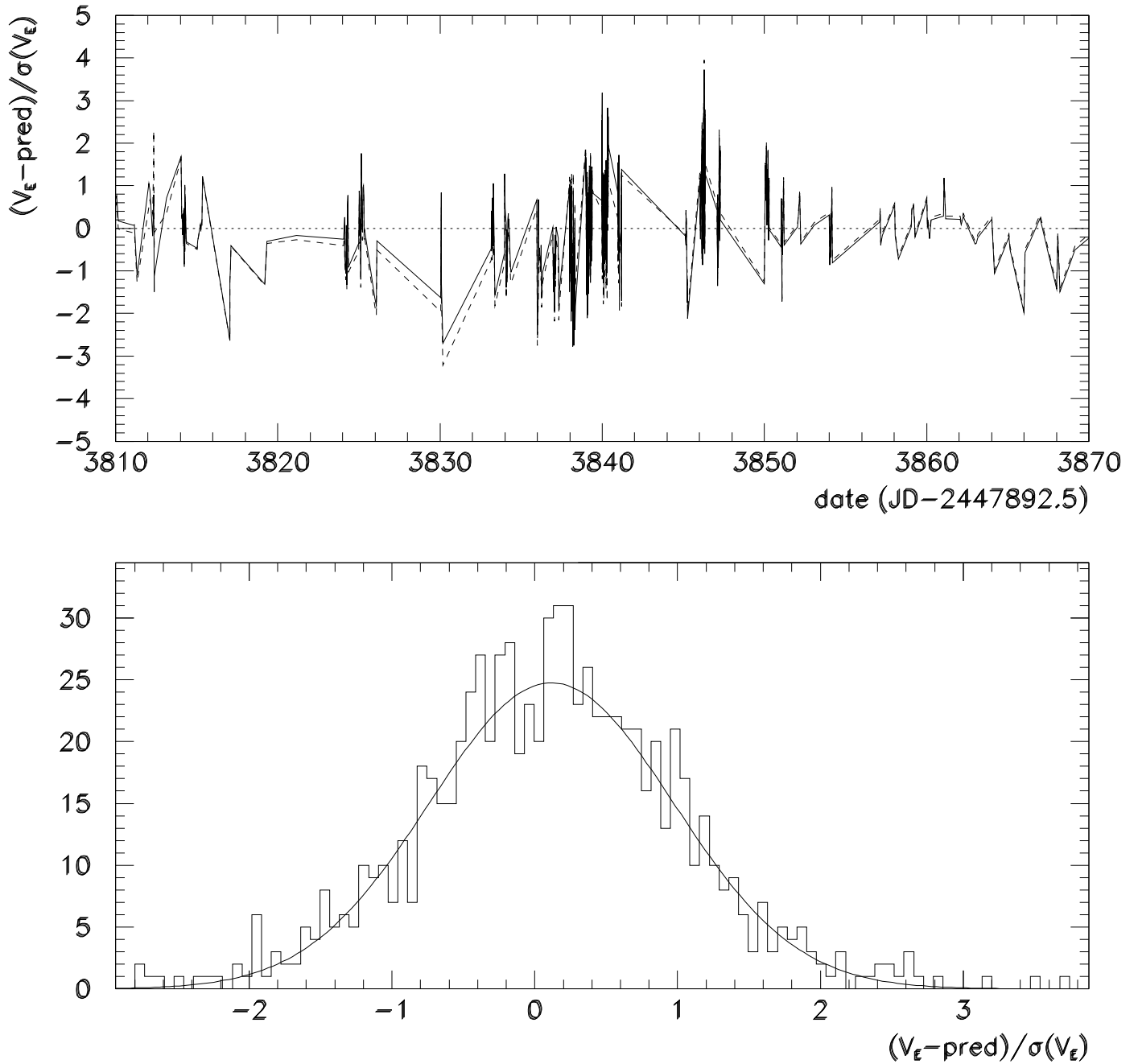


**Fig. 6.** Normalized residuals of EROS  $V_E$  data. Top: residuals as a function of time. The solid line is model 1 (model 2 is not shown, but similar) and the dashed line is An et al. (2002) lens model. The residuals of both models do not show any obvious trend as a function of time. Bottom: distribution of residuals for model 1. The line shows the fit to a gaussian.